

Copper(II) Complexes of Novel *N*-Alkylated Derivatives of *cis,cis*-1,3,5-Triaminocyclohexane. 1. Preparation and Structure

Gyungse Park,[†] Junlong Shao,[†] Frances H. Lu,[‡] Robin D. Rogers,[§] N. Dennis Chasteen,[†] Martin W. Brechbiel,[‡] and Roy P. Planalp^{*†}

Departments of Chemistry, University of New Hampshire, Durham, New Hampshire 03824, and The University of Alabama, Tuscaloosa, Alabama 35487, and Chemistry Section, Radiation Oncology Branch, National Institutes of Health, Building 10, Room B3-B69, Bethesda, Maryland 20892

Received July 21, 2000

Novel *N,N',N''*-trialkylated derivatives of *cis,cis*-1,3,5-triaminocyclohexane (tach), designated tach-R₃, were prepared through alkylation of *N*-protected tach with subsequent acid deprotection, to afford *N*-methyl, *N*-ethyl, and *N*-*n*-propyl derivatives as their trihydrobromide salts. The tach-neopentyl₃ and tach-furan₃ derivatives were prepared by formation of the imine from tach and pivaldehyde or furan-2-carboxaldehyde, respectively, followed by reduction of the imine. Complexes [Cu(tach-R₃)Cl₂] (R = Me, Et, *n*-Pr, CH₂-2-thienyl, and CH₂-2-furanyl) were prepared from CuCl₂ in MeOH or MeOH–Et₂O solvent. Crystallographic characterization of [Cu(tach-Et₃)Br_{0.8}Cl_{1.2}] (*Pnma*, *a* = 8.2265(1) Å, *b* = 12.5313(1) Å, *c* = 15.3587(3) Å, *Z* = 4) reveals a square-based pyramidal CuN₃X₂ coordination sphere in which one nitrogen donor occupies the apical position at a slightly longer distance (Cu–N = 2.218(5) Å) than those of the basal nitrogens (Cu–N = 2.053(2) Å). The solution-phase (pH 7.4 buffered and methanol) and solid-phase structures of [Cu(tach-R₃)Cl₂] have been studied extensively by EPR and visible–near-IR spectroscopies. The square-based pyramidal structure is retained in solution, according to correspondence of solution and solid-state data. In aqueous solution, halide is replaced by water, as indicated by the high-energy UV–vis spectral shifts and bonding parameters of [Cu(tach-Et₃)]²⁺(aq) derived from EPR data. The proposed aqueous-phase species, in the pH range 7.4 to 10.1, is [Cu(tach-Et₃)(H₂O)₂]²⁺. The complex [Cu(tach-Me₃)]²⁺(aq) does not appear to dimerize or form metal–hydroxo species at pH 7.4, in contrast to other Cu(II)–triamine complexes, e.g., [Cu(1,4,7-triazacyclononane)]²⁺(aq) and [Cu(tach-H₃)]²⁺(aq) (the complex of unalkylated tach). This difference is attributed to the steric effect of the *N*-alkyl groups in the tach-R₃ series.

Introduction

Copper possesses a rich coordination chemistry that is reflected in its many biological and synthetic roles.^{1–4} Copper complexes catalyze many reactions, including hydrolysis, Diels–Alder, and redox reactions. Copper(II) complexes that can catalyze hydrolysis reactions of phosphate and amide linkages are interesting as synthetic polynucleotide or peptide cleavage agents. Although metal-catalyzed polynucleotide and peptide cleavage reactions have been known for some time,^{5,6} interest is turning to complexes with more labile active sites, such as those of Cu(II) and the lanthanides, that may achieve greater substrate turnover.⁷

Many Cu(II) complexes are known to cleave phosphodiester bonds and, to a lesser degree, amide bonds.^{8,9} Tridentate amine ligands have been generally effective supports of Cu(II), as they allow several open metal coordination sites. Detailed mechanistic studies of Cu(II)–[9]aneN₃ ([9]aneN₃ = 1,4,7-triazacyclononane) complexes by Burstyn et al. have led to a number of insights into these processes.^{7,10,11} Several other trinitrogen ligands, whose copper complexes catalyze phosphate diester cleavage and transesterification, have also received careful mechanistic study.^{12–14} However, many details of these processes remain unclear or contradictory, underscoring the complexity of the chemistry involved.

We have initiated studies of the structure, electronic properties, and reactivity of a number of biologically relevant copper complexes that serve as hydrolytic cleavage agents. It is important to understand the solution coordination geometries and electronic structures of metal complexes that are potentially active species or precursors to such species. It is believed that

* Corresponding author. Phone: (603) 862-2471. Fax: (603) 862-4278. E-mail: roy.planalp@unh.edu.

[†] University of New Hampshire.

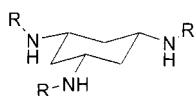
[‡] National Institutes of Health.

[§] The University of Alabama.

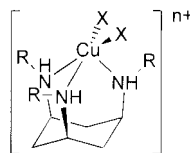
- (1) Cotton, F. A.; Wilkinson, G.; Murillo, C. A.; Bochmann, M. *Advanced Inorganic Chemistry*; Wiley: New York, 1999; pp 873 ff.
- (2) Evans, D. A.; Barnes, D. M.; Johnson, J. S.; Lectka, T.; von Matt, P.; Miller, S. J.; Murry, J. A.; Norcross, R. D.; Shaughnessy, E. A.; Campos, K. R. *J. Am. Chem. Soc.* **1999**, *121*, 7582.
- (3) Evans, D. A.; Miller, S. J.; Lectka, T.; von Matt, P. *J. Am. Chem. Soc.* **1999**, *121*, 7559.
- (4) Hathaway, B. Copper. In *Comprehensive Coordination Chemistry*; Wilkinson, G., Gillard, R. D., McCleverty, J. A., Eds.; Pergamon: London, 1987; Vol. 5, Chapter 53.4 ff.
- (5) Gustafson, R. L.; Martell, A. E. *J. Am. Chem. Soc.* **1962**, *84*, 2309.
- (6) Chin, J.; Banaszczuk, M.; Jubian, V.; Zou, X. *J. Am. Chem. Soc.* **1989**, *111*, 186.
- (7) Hegg, E. L.; Burstyn, J. N. *Coord. Chem. Rev.* **1998**, *173*, 133.

- (8) Reddy, K. V.; Jacobson, A. R.; Kung, J. I.; Sayre, L. M. *Inorg. Chem.* **1991**, *30*, 3520.
- (9) Sayre, L. M.; Reddy, K. V.; Jacobson, A. R.; Tang, W. *Inorg. Chem.* **1992**, *31*, 935.
- (10) Deal, K. A.; Burstyn, J. N. *Inorg. Chem.* **1996**, *35*, 2792.
- (11) Hegg, E. L.; Burstyn, J. N. *J. Am. Chem. Soc.* **1995**, *117*, 7015.
- (12) Wahnou, D.; Hynes, R. C.; Chin, J. *J. Chem. Soc., Chem. Commun.* **1994**, 1441.
- (13) Itoh, T.; Hisada, H.; Sumiya, T.; Hosono, M.; Usui, Y.; Fujii, Y. *J. Chem. Soc., Chem. Commun.* **1997**, 677.
- (14) Itoh, T.; Hisada, H.; Usui, Y.; Fujii, Y. *Inorg. Chim. Acta* **1998**, *283*, 51.

Chart 1



R = Me: tach-Me₃
 R = Et: tach-Et₃
 R = *n*-Pr: tach-Pr₃
 R = CH₂-2-thienyl: tach-thioph₃
 R = CH₂-2-furanyl: tach-furan₃
 R = CH₂-*t*-Bu: tach-neopentyl₃



R = Me, Et, *n*-Pr, CH₂-2-thienyl
 and CH₂-2-furanyl, X = Cl, n = 0.
 R = Et, X₂ = (Br)_{0.8}(Cl)_{1.2}, n = 0.
 R = Et, X = (H₂O), n = 2.

the active species involve association of the substrate to one or more Lewis acidic metal(s), followed by the addition of a nucleophile, generally hydroxide although others have been postulated.¹¹ The formation of the active species from the precursor generally involves the steps of replacement of coordinated halide by water, followed by hydrolysis of the resulting aqua compounds to form a coordinated hydroxo group that acts as nucleophile for phosphate cleavage. Therefore, these studies have the long-term goal of better understanding the mechanism of hydrolysis for the purposes of developing more effective hydrolysis agents.

In the present work, we focus on Cu(II) complexes of *N,N',N''*-trialkyltach (tach = *cis,cis*-1,3,5-triaminocyclohexane) (Chart 1). We have observed that aqueous [Cu(tach-R₃)X₂] (X = Cl, Br) cleaves *p*-nitrophenyl phosphate diesters with rates that slightly exceed those of [Cu(9)aneN₃]Cl₂.¹⁵ We are therefore exploring the interaction of Cu(II) with tach-R₃ and reactivity of the resulting complexes. Tach, in the closed conformation, is known to bind a variety of metals in a facial geometry,^{16–18} but relatively little is known concerning the effects of the addition of *N*-alkyl groups on coordination properties of tach. The properties of unalkylated tach (also designated “tach-H₃” to distinguish from tach-R₃, where R ≠ H) have been studied by Fujii et al., who observed cleavage of 2,4-dinitrophenyl phosphate esters by complexes formed from Cu(II) and tach-H₃ in situ.¹⁴ We draw on our recent synthesis of tach-H₃ and tach-R₃ to overcome limitations on the availability of the ligands.^{19,20}

Herein we report the synthesis of an array of *N*-substituted-tach–Cu(II)–dihalide complexes and corresponding new tach ligands and the determination of their solid-state and solution structures. We have analyzed the hydrolysis of these dihalides and assigned a structure of the resulting aquo species. In the following paper,¹⁵ we report their hydrolysis activity toward

phosphate diesters and implications of the observed kinetics for the mechanism of hydrolysis.

Experimental Section

Materials and Methods. Anhydrous grade MeOH was obtained from Fisher Scientific. Et₂O was distilled from Na/K. Anhydrous grade DMSO and DMF were obtained from Aldrich. Dipropyl sulfate was purchased from TCI America. All other reagents were from Aldrich, Sigma, or Fluka. Tach·3HBr,¹⁹ tach-thioph₃,¹⁸ tach-Me₃,²⁰ and tach-Et₃²⁰ were prepared as previously reported. ⁶³Cu was obtained from Cambridge Isotope Laboratories.

¹H and ¹³C NMR were obtained using a Varian Gemini 300 instrument or a Bruker AM360 instrument. Chemical shifts are reported in ppm on the δ scale relative to TMS, TSP, or solvent. Proton chemical shifts are annotated as follows: ppm (multiplicity, integral, coupling constant (Hz)). Chemical ionization mass spectra (CI-MS) were obtained on a Finnegan 3000 instrument. Fast atom bombardment (FAB-MS) mass spectra were taken on a Extrel 4000. Elemental analysis was performed by Atlantic Microlabs (Atlanta, GA) or by Galbraith Laboratories (Knoxville, TN).

EPR and Visible–Near-IR Spectroscopy. X-band (9.15 GHz) EPR spectra were measured on a laboratory assembled spectrometer equipped with a Bruker ER 041 XK-H microwave bridge and a Varian TE₁₀₂ cavity fitted with a liquid nitrogen Dewar insert as described elsewhere.²¹ Q-band (35 GHz) spectra were measured on a Varian E-9 spectrometer. The E-110 Q-band microwave bridge was modified with a Quinstar Technology QLN-3635-AA low noise microwave amplifier, giving a ~7-fold improvement in signal/noise ratio at –13 dB microwave power attenuation. A 20 dB directional coupler was inserted in the microwave circuit for counting the frequency. A 10 dB isolator was placed between the EIP model 448 A frequency counter and the coupler to eliminate feedback interference to the microwave bridge from the counter. A fabricated ribbon-wound cylindrical TE₀₁₁ cavity²² immersed in a stream of cold dinitrogen gas was employed for Q-band measurements at 100 K. Samples were contained in calibrated 3 mm i.d.–4 mm o.d. quartz sample tubes for X-band measurements on frozen solutions at 77 K and in 1.3 mm i.d.–2.0 mm o.d. quartz capillary tubing for Q-band measurements at 100 K. A quartz flat cell was used for room-temperature measurements on aqueous solutions at X-band. For accurate *g*-factor determinations, the X-band microwave frequency was determined using a Hewlett-Packard model 5350A counter and the field calibrated with either a MicroNow model 515 NMR gaussmeter or a standard sample of Mn²⁺ in CaO (*g* = 2.0011(1) with field separations of 8.627(4), 25.881(4), and 43.113(4) mT between the *M*_l = ±1/2, ±3/2, and ±5/2 pairs of lines, respectively).²³ The CaO sample was blended with a trace amount of coal (*g* = 2.0035(1)) to give a central *g*-mark in the EPR spectrum and sealed under vacuum. Spectrometer settings for X-band frozen solutions were the following: microwave power = 5 mW; modulation amplitude = 0.2 mT at 100 kHz; scan time = 500 s; time constant = 0.3 s; frequency = 9.1500 GHz; scan range = 100 mT. Room-temperature X-band spectra were obtained with the following settings: microwave power = 10 mW; modulation amplitude = 0.5 mT; scan time = 1000 s; time constant = 1 s; scan range = 100 mT; frequency = 9.5284 GHz. The spectrometer settings for Q-band spectra were the following: microwave power = 190 μW; modulation amplitude = 0.2 mT; scan time = 16 min; time constant = 1 s; scan range = 200 mT; frequency = 34.8 GHz.

Aqueous samples for frozen solution EPR measurements were prepared in 50 mM Hepes buffer/glycerol, pH 7.4 solution (2:1 v:v), or in 50 mM Caps buffer/glycerol, pH 10.1 (2:1 v:v). The spectra of the complex [Cu(tach-Me₃)Cl₂] in 50 mM HEPES buffer and 50 mM HEPES/glycerol (2:1 v/v) were identical, suggesting that coordination of glycerol to Cu(II) does not occur in the mixed solvent. Ligand-field spectra of 5 mM complex in analytical grade methanol or 50 mM HEPES buffer, pH 7.4, were measured in 1 cm quartz cuvettes on a Varian Cary-5 UV/vis/NIR spectrophotometer. Spectra of solid samples

(15) Deal, K. A.; Park, G.; Shao, J.; Chasteen, N. D.; Planalp, R. P.; Brechbiel, M. W. *Inorg. Chem.* **2001**, *40*, 4176.

(16) Lions, F.; Martin, K. V. *J. Am. Chem. Soc.* **1957**, *79*, 1572.

(17) Hegetschweiler, K.; Kradolfer, T.; Gramlich, V.; Hancock, R. D. *Chem. Eur. J.* **1995**, *1*, 74.

(18) Ye, N.; Rogers, R. D.; Brechbiel, M. W.; Planalp, R. P. *Polyhedron* **1998**, *17*, 603.

(19) Bowen, T.; Planalp, R. P.; Brechbiel, M. W. *Bioorg. Med. Chem. Lett.* **1996**, *6*, 807.

(20) Park, G.; Lu, F. H.; Ye, N.; Brechbiel, M. W.; Torti, S. V.; Torti, F. M.; Planalp, R. P. *JBIC* **1998**, *3*, 449.

(21) Yang, X.; Chasteen, N. D. *Biophys. J.* **1996**, *71*, 1587.

(22) Wang, W.; Chasteen, N. D. *J. Magn. Reson.* **1996**, *116*, 237.

(23) Shao, J.; Grady, J. K.; Chasteen, N. D. *EPR Newslett.* **1999**, *10*, 7.

were obtained on powders blended in a KBr pellet. Spectra gathered linearly in wavelength were converted to a wavenumber scale and least-squares fitted to a sum of Gaussian functions using the software program Origin 6.0 (MicroCal, Inc.).

Ligand Syntheses.

***N,N',N''*-Tripropyl-1,3,5-*cis,cis*-triaminocyclohexane-*N,N',N''*-tri-*p*-toluenesulfonyl Amide (tach-Ts₃Pr₃).** 1,3,5-*cis,cis*-Triaminocyclohexane-*N,N',N''*-tri-*p*-toluenesulfonyl amide²⁰ (10.69 g, 18.09 mmol) was dissolved in dry DMF (150 mL), cooled with an ice bath, and NaH (87 mmol) was added. After H₂ evolution had ceased, dipropyl sulfate (36.4 g, 0.200 mmol) was added. The reaction mixture was then heated to ca. 90 °C for 18 h. After cooling, concentrated NH₄OH/H₂O (1:1) (150 mL) was added and the reaction was stirred for 1 h. The solvents were removed by high-vacuum rotary evaporation. The residue was taken up in EtOAc (500 mL), washed with salt solution (100 mL), dried over Na₂SO₄, filtered, and concentrated to the crude solid product. The pure product was isolated by column chromatography on silica, eluting with CHCl₃ (100%). After solvent removal, the product was isolated as a white solid (5.3 g, 40%): ¹H NMR (CDCl₃) δ 7.64 (d, 2H, *J* = 7.8) 7.29 (d, 2H, *J* = 7.8), 3.50 (m, 1H), 2.98 (t, 2H, *J* = 7.8), 2.43 (s, 3H), 1.70–1.40 (m, 4H), 0.83 (t, 1H, *J* = 6.6); ¹³C NMR (CDCl₃) δ 143.42, 138.26, 129.88, 126.85, 54.90, 46.89, 35.65, 24.24, 21.39, 11.06; MS (CI/NH₃) 735 (M⁺ + 1). Anal. Calcd for C₃₆H₅₁N₃O₆S₃: C, 60.02; H, 7.17; N, 5.85. Found: C, 59.97; H, 7.28; N, 5.85.

***N,N',N''*-Tripropyl-1,3,5-*cis,cis*-triaminocyclohexane Trihydrobromide (tach-Pr₃·3HBr).** A flask was charged with acetic anhydride (ACS reagent grade, 98%) (16.55 mL) and cooled in an ice bath. Concentrated HBr (40.83 mL) was added slowly, and the solution was allowed to stir at room temperature for 18 h. tach-Ts₃Pr₃ (5.0 g, 7.0 mmol) was added, and the suspension was refluxed for 24 h during which a dark red-brown solution formed. The solution was rotary evaporated to leave a dark solid which was taken up in H₂O (25 mL) and extracted with Et₂O (2 × 50 mL). The aqueous layer was filtered and concentrated to ca. 10 mL. This residue was taken up in 100% EtOH (ca. 50 mL), and an equal amount of Et₂O was added to precipitate the product. The white suspension was cooled at 4 °C for 18 h, and then the solid was collected, washed with Et₂O, and dried under vacuum (3.2 g, 92%): ¹H NMR (D₂O) δ 3.47 (tt, 1H, *J* = 11.7, 3.5), 3.11 (t, 2H, *J* = 7.8), 2.64 (br d, 1H, *J* = 10.8), 1.80–1.59 (m, 3H), 1.00 (t, 3H, *J* = 7.8); ¹³C NMR (D₂O) δ 54.82, 49.85, 32.97, 22.28, 13.11; MS (CI/NH₃) 256 (M⁺ + 1). Anal. Calcd for C₁₅H₃₃N₃·(HBr)₃: C, 36.14; H, 6.69; N, 8.43. Found: C, 36.27; H, 6.71; N, 8.34.

1,3,5-*cis,cis*-Triaminocyclohexane-*N,N',N''*-tris(neopentyl-imine). Tach·3HBr (2.0 g, 5.4 mmol) was dissolved in H₂O (10 mL) with NaOH (0.695 g, 16.1 mmol) to form a clear solution. Benzene (150 mL) was added, and the water was removed by azeotropic distillation with a Dean–Stark trap. Pivaldehyde (1.39 g, 16.1 mmol) was added during this process, which was then continued for 12 h. After cooling, the solution was decanted and rotary evaporated to a white solid (1.57 g, 87%): ¹H NMR (CDCl₃) δ 7.56 (s, 1H), 3.18 (m, 1H), 1.70 (q, 1H, *J* = 11.7), 1.63 (m, 1H), 1.04 (s, 9H); ¹³C NMR (CDCl₃) δ 170.14, 65.71, 40.81, 35.71, 26.85; MS (CI/NH₃) 334 (M⁺ + 1). Anal. Calcd for C₂₁H₃₉N₃: C, 75.60; H, 11.80; N, 12.60. Found: C, 75.79; H, 11.73; N, 12.32.

***N,N',N''*-Trineopentyl-1,3,5-*cis,cis*-triaminocyclohexane (tach-neopentyl₃).** The above imine (2.00 g, 6.01 mmol) was dissolved in MeOH (100 mL), and NaBH₄ (1.37 g, 3.67 mmol) was added. The reaction mixture was stirred for 12 h after which the solvent was removed by rotary evaporation. The residue was taken up in CHCl₃ (100 mL) and stirred vigorously with a 1:1 mixture of saturated salt solution and 5% NaHCO₃ (100 mL). The layers were separated, and the CHCl₃ solution was washed with saturated salt solution (2 × 100 mL), dried over Na₂SO₄, filtered, and rotary evaporated to leave the product (1.89 g, 93%): ¹H NMR (CD₃OD) δ 4.88 (s, 1H), 2.51 (tt, 1H, *J* = 11.7, 3.9), 2.43 (s, 2H), 2.18 (br d, 1H, *J* = 12.0), 1.03 (q, 1H, *J* = 11.7), 0.94 (s, 9H); ¹³C NMR (CD₃OD) δ 60.38, 56.62, 39.31, 32.15, 28.32; MS (CI/NH₃) 340 (M⁺ + 1). Anal. Calcd for C₂₁H₄₅N₃: C, 74.25; H, 13.38; N, 12.37. Found: C, 74.28, H, 13.20, N, 12.28.

1,3,5-*cis,cis*-Triaminocyclohexane-*N,N',N''*-tris(2-methylfuran-imine). tach·3HBr (4.0 g, 10.8 mmol) was dissolved in H₂O (10 mL)

with NaOH (1.29 g, 32.2 mmol) to form a clear solution. Benzene (150 mL) was added, and the water was removed by azeotropic distillation with a Dean–Stark trap. Furfural (3.097 g, 32.25 mmol) was added during this process and then continued for 12 h. After cooling, the solution was decanted and rotary evaporated to an oil (3.36 g, 86%): ¹H NMR (CDCl₃) δ 8.17 (s, 1H), 7.520 (d, 1H, *J* = 0.9), 6.74 (d, 1H, *J* = 3.3), 6.48 (dd, 1H, *J* = 3.3, 1.8), 3.50 (tt, 1H, *J* = 11.4, 3.9), 2.07 (q, 1H, *J* = 12.0), 1.91 (br d, 1H, *J* = 12.0); ¹³C NMR (CDCl₃) δ 151.58, 148.30, 144.90, 114.46, 111.60, 66.53, 40.67; MS (CI/NH₃) 364 (M⁺ + 1). Anal. Calcd for C₂₁H₂₁N₃O₃: C, 72.59; H, 6.10; N, 12.10. Found: C, 72.41; H, 6.04; N, 11.98.

1,3,5-*cis,cis*-Triaminocyclohexane-*N,N',N''*-tris(methylenefuran) (tach-furan₃). The above imine (3.00 g, 8.26 mmol) was dissolved in MeOH (100 mL) and treated with NaBH₄ (1.23 g, 32.25 mmol) as described for tach-neopentyl₃. Workup afforded the product as an oil (2.68 g, 88%): ¹H NMR (CDCl₃) δ 7.36 (s, 1H), 6.31 (m, 1H), 6.16 (d, 2H, *J* = 3.3), 3.80 (s, 2H), 2.54 (tt, 1H, *J* = 10.8, 3), 2.15 (d, 1H, *J* = 11.7), 1.70 (br s, 1H), 0.96 (q, 1H, *J* = 11.7); ¹³C NMR (CDCl₃) δ 153.92, 141.867, 110.15, 106.81, 52.66, 43.22, 39.66; MS (CI/NH₃) 370 (M⁺ + 1). Anal. Calcd for C₂₁H₂₇N₃O₃: C, 68.26; H, 7.38; N, 11.37. Found: C, 68.26; H, 7.52; N, 11.43.

Metal Complex Syntheses. [Cu(tach-Me₃)Cl₂]. A mixture of tach-Me₃·3HBr (0.12 g, 0.29 mmol) in water (5 mL), Na₂CO₃·H₂O (0.054 g, 0.44 mmol, 1.5 equiv) in water (5 mL), and benzene (100 mL) was stirred and heated in a 250 mL round-bottomed flask fitted with a Dean–Stark trap with a water-cooled condenser. Benzene–water azeotrope was distilled for 14 h with collection of ca. 11.7 mL of water. The benzene layer was transferred to another 250 mL round-bottomed flask and dried under reduced pressure to give tach-Me₃ as a white solid. The solid was dissolved in a mixture of CHCl₃ (2 mL) and Et₂O (4 mL) and added to a green solution of CuCl₂ (0.040 g, 0.29 mmol) in a mixture of MeOH/Et₂O (2 mL/4 mL) affording a green precipitate immediately. Decanting the supernatant and extracting the solid with CH₂Cl₂ (5 mL) followed by drying under reduced pressure afforded the product as a green solid (0.056 g, 0.18 mmol, 63%). Anal. Calcd for C₉H₂₁N₃CuCl₂ (Cu(tach-Me₃)Cl₂): C, 35.36; H, 6.92; N, 13.74. Found: C, 35.16; H, 6.85; N, 13.62. UV (MeOH): 687 nm (ε = 111.7). MS (FAB/DMSO/glycerol): 234 (M – 2Cl[−]).

[Cu(tach-Et₃)Br_{0.8}Cl_{1.2}]. An aqueous solution (3 mL) of tach-Et₃·3HBr (0.193 g, 0.426 mmol) was neutralized by adding 12.8 mL of 0.100 N NaOH solution (0.103 mmol, 3 equiv). The neutralized ligand was dried under reduced pressure for 10 h and extracted into CHCl₃ (12 mL). This solution was filtered and dried under reduced pressure. The resulting pale-yellow solid was taken up in CHCl₃ (3 mL) and added to a pale green solution of CuCl₂ (0.0573 g, 0.426 mmol) in anhydrous MeOH (2 mL) affording a dark green solution. The dark green solution was filtered and dried under reduced pressure. The dried crude product was dissolved in anhydrous MeOH (5 mL), and anhydrous Et₂O was diffused into MeOH solution yielding green microcrystals (0.0541 g, 0.156 mmol, 35.5%). The average proportions of Br and Cl are indicated by the elemental analysis; however, X-ray crystallographic analysis of a particular crystal of this material indicated the composition [Cu(tach-Et₃)Br_{0.8}Cl_{1.2}] (see below). Anal. Calcd for C₁₂H₂₇Br_{0.7}Cl_{1.3}CuN₃ (Cu(tach-Et₃)Br_{0.7}Cl_{1.3} (specific proportion Br:Cl varies): C, 38.04; H, 7.18; N, 11.09. Found: C, 38.47; H, 6.71; N, 10.45. UV (MeOH): 716 nm (ε = 132.8). MS (FAB/glycerol): 276 (M – 2X[−]).

[Cu(tach-Et₃)Cl₂]. A mixture of tach-Et₃·3HBr (0.17 g, 0.37 mmol) in water (5 mL), Na₂CO₃·H₂O (0.073 g, 0.59 mmol, 1.6 equiv) in water (5 mL), and benzene (100 mL) was stirred and heated in a 250 mL round-bottomed flask fitted with a Dean–Stark trap with a water-cooled condenser. Benzene–water azeotrope was distilled for 14 h with collection of ca. 11.9 mL of water. The benzene layer was dried under reduced pressure to give tach-Et₃ as a white solid. A pale yellow solution of tach-Et₃ (0.079 g, 0.37 mmol) in a mixture of MeOH (2 mL) and Et₂O (4 mL) was added to a pale green solution of CuCl₂ (0.050 g, 0.37 mmol) in a mixture of MeOH (3 mL) and Et₂O (6 mL) producing a dark green solution and a brown precipitate. The brown precipitate was filtered away, and the dark green filtrate was dried under reduced

pressure affording a green solid. The green solid was dissolved in CH_2Cl_2 (4 mL), and Et_2O was diffused into the solution affording green prisms (0.053 g, 0.15 mmol, 43%). Anal. Calcd for $\text{C}_{12}\text{H}_{27}\text{N}_3\text{CuCl}_2$ ($[\text{Cu}(\text{tach-Et}_3)\text{Cl}_2]$): C, 41.44; H, 7.82; N, 12.08. Found: C, 41.22; H, 7.83; N, 11.94. UV (MeOH): 718 nm ($\epsilon = 97.0$). MS (FAB/glycerol): 276 ($M - 2\text{Cl}^-$).

[Cu(tach-Pr₃)Cl₂]. A mixture of tach-Pr₃·3HBr (0.250 g, 0.505 mmol) in water (5 mL), $\text{Na}_2\text{CO}_3 \cdot \text{H}_2\text{O}$ (0.100 g, 0.808 mmol, 1.6 equiv) in water (5 mL), and benzene (100 mL) was stirred and heated in a 250 mL round-bottomed flask fitted with Dean–Stark trap with a water-cooled condenser. Benzene–water azeotrope was distilled for 14 h with collection of ca. 11.7 mL of water. The benzene layer was dried under reduced pressure to give tach-Pr₃ as a white solid. To a pale green solution of CuCl_2 (0.0678 g, 0.505 mmol) in a mixture of MeOH (2 mL) and Et_2O (6 mL) was added a pale yellow solution of neutralized tach-Pr₃ (0.127 g, 0.505 mmol) in a mixture of MeOH (2 mL) and Et_2O (6 mL) affording a dark green solution. Turquoise, featherlike crystals formed upon standing and were isolated by decanting the supernatant. The crystals were dried under reduced pressure, extracted into CH_2Cl_2 (5 mL) and filtered, and dried again under reduced pressure to afford the turquoise product (0.140 g, 0.363 mmol, 72%). Anal. Calcd for $\text{C}_{15}\text{H}_{33}\text{N}_3\text{CuCl}_2$ ($[\text{Cu}(\text{tach-Pr}_3)\text{Cl}_2]$): C, 46.21; H, 8.53; N, 10.78. Found: C, 46.33; H, 8.36; N, 10.63. UV (MeOH): 703 nm ($\epsilon = 95.9$). MS (FAB/glycerol/DMSO/EtOH): 318 ($M - 2\text{Cl}^-$).

[Cu(tach-furan₃)Cl₂]. A yellowish solution of tach-furan₃ (0.0549 g, 0.149 mmol) in MeOH (2 mL) was added to a green solution of CuCl_2 (0.0209 g, 0.154 mmol) in MeOH (2 mL) affording a deep green solution. Diethyl ether was diffused into the mixture solution for 5 days yielding green crystals and a yellow-green powder. Decanting the supernatant and extraction with CH_2Cl_2 (5 mL) followed by Et_2O diffusion into the CH_2Cl_2 solution afforded green prisms. The prisms were isolated by filtration and dried under reduced pressure. Yield: 0.0321 g (0.0637 mmol, 42.8%). Anal. Calcd for $\text{C}_{21}\text{H}_{27}\text{N}_3\text{Cl}_2\text{CuO}_3$ ($[\text{Cu}(\text{tach-furan}_3)\text{Cl}_2]$): C, 50.05; H, 5.40; N, 8.34. Found: C, 49.84; H 5.39; N, 8.22. UV (MeOH): 700 nm ($\epsilon = 100.9$). MS (FAB/DMSO/glycerol): 432 ($M - 2\text{Cl}^-$).

In Situ Preparations of $[\text{Cu}(\text{tach-R}_3)]^{2+}$ in Aqueous or Aqueous/Alcoholic Media.

[Cu(tach-Me₃)²⁺]. A colorless solution of 0.100 M tach-Me₃·3HBr in water (1.50 mL) (prepared by neutralization of tach-Me₃·3HBr (0.0621 g, 0.150 mmol) in water (1.036 mL) with 3 equiv of 1.02 N NaOH (0.464 mL)) was added to a blue solution of 0.100 M CuCl_2 in water (1.49 mL), affording a deep blue 50 mM $[\text{Cu}(\text{tach-Me}_3)]^{2+}$ solution. Occasionally, a faint blue-green precipitate formed, presumably insoluble Cu(II) hydroxide, which was removed by filtration. From this stock solution was prepared a 5 mM $[\text{Cu}(\text{tach-Me}_3)]^{2+}$ solution by further dilution with a mixture of 50 mM HEPES/glycerol (2:1), pH 7.4, at 25 °C.

⁶³CuCl₂/DCl. A ca. 10 mg amount of ⁶³Cu metal was dissolved in 6 N HNO_3 and the resulting solution evaporated to dryness under a stream of dry nitrogen gas. The solid copper nitrate was dissolved in sufficient 0.01 N DCl to provide a 20 mM solution of ⁶³Cu(II).

Tach-Me₃·3DCl. A clear solution of tach-Me₃·3HBr (0.033 g, 80 μmol) in D_2O was treated with DCl (1 mL of 37% w/w in D_2O), and dried under reduced pressure affording a white solid. The procedure was repeated two more times giving the product tach-Me₃·3DCl as a white solid. FT-IR: 2100 cm^{-1} (N–D).

⁶³Cu(tach-Me₃)²⁺. A pale blue solution of 20 mM ⁶³CuCl₂/DCl (0.25 mL, 5.0 μmol) was added to a clear solution of tach-Me₃·3DCl (0.014 g, 5.0 μmol) in a mixture of 50 mM HEPES/glycerol-*d*₃ (2:1), pH 7.4, at 25 °C (0.75 mL), affording 5 mM $[\text{Cu}(\text{tach-Me}_3)]^{2+}$.

[Cu(tach-Et₃)²⁺]. To a blue solution of CuCl_2 (0.0201 g, 0.150 mmol) in water (1.5 mL) was added a clear solution of tach-Et₃·3HBr, neutralized by 3 equiv of 1.0 N NaOH (0.0681 g, 0.150 mmol) in water (1.5 mL) to form a blue $[\text{Cu}(\text{tach-Et}_3)]^{2+}$ solution with a small amount of faint blue-green precipitate, presumably insoluble Cu(II) hydroxides, which was removed by filtration. From this stock solution was prepared a 5 mM $[\text{Cu}(\text{tach-Et}_3)]^{2+}$ solution by further dilution with a mixture of 50 mM HEPES/glycerol (2:1), pH 7.4, at 25 °C.

[Cu(tach-Pr₃)²⁺]. The turquoise solid $[\text{Cu}(\text{tach-Pr}_3)\text{Cl}_2]$ (0.012 g, 0.30 mmol) was dissolved in a mixture of 50 mM HEPES/glycerol

Table 1. Crystal Data and Structure Refinement for $[\text{Cu}(\text{tach-Et}_3)\text{Br}_{0.8}\text{Cl}_{1.2}]$

empirical formula	$\text{C}_{12}\text{H}_{27}\text{Br}_{0.8}\text{Cl}_{1.2}\text{CuN}_3$
fw	383.37
temp	173(2) K
cryst system	orthorhombic
space group	<i>Pnma</i>
a	8.2265(1) Å
b	12.5313(1) Å
c	15.3587(3) Å
V	1583.31(4) Å ³
Z	4
d(calcd)	1.608 Mg/m ³
abs coeff	3.589 mm ⁻¹
F(000)	790
cryst size	0.10 × 0.16 × 0.32 mm
θ_{range} for data collcn	2.10–27.86°
reflens colld	9500
indepdt reflcns	1952 ($R_{\text{int}} = 0.0411$)
obsd reflcns	1551 ($[I > 2\sigma(I)]$)
abs corr	SADABS
range of relat transm factors	0.97 and 0.68
data/restraints/params	1948/0/100
goodness-of-fit on F^2	1.070
SHELX-93 weight params	0.0461, 1.3522
final R indices $[I > 2\sigma(I)]$	$R1 = 0.0413$, $wR2 = 0.0900$
R indices (all data)	$R1 = 0.0596$, $wR2 = 0.1000$
extinction coeff	0.0017(5)
largest diff peak and hole	0.614 and $-0.594 \text{ e} \text{ \AA}^{-3}$

(2:1) (3 mL), pH 7.4, at 25 °C, affording a suspension which clarified to turquoise 5 mM $[\text{Cu}(\text{tach-Pr}_3)]^{2+}$ upon addition of MeOH (3 mL).

[Cu(tach-thioph₃)²⁺]. The green solid $[\text{Cu}(\text{tach-thioph}_3)\text{Cl}_2]$ ¹⁸ (0.017 g, 30 μmol) was dissolved in a mixture 50 mM HEPES/glycerol (2:1) (3 mL), pH 7.4, at 25 °C, affording a green cloudy solution which became a clear green 5 mM $[\text{Cu}(\text{tach-thioph}_3)]^{2+}$ solution by adding EtOH (3 mL).

X-ray Data Collection, Structure Solution, and Refinement for $[\text{Cu}(\text{tach-Et}_3)\text{Br}_{0.8}\text{Cl}_{1.2}]$. Crystals of $[\text{Cu}(\text{tach-Et}_3)\text{Br}_{0.8}\text{Cl}_{1.2}]$ suitable for study were obtained by vapor phase diffusion of Et_2O into a CH_2Cl_2 solution of product. A fragment was taken directly from the crystals in supernatant, sealed in epoxy, and mounted on a glass fiber. Data were collected on a Siemens SMART/CCD area detector diffractometer ($-10 \leq h \leq 10$, $-16 \leq k \leq 13$, $-14 \leq l \leq 20$; $2.10 \leq \theta \leq 27.86^\circ$) at -100°C with graphite-monochromated Mo $K\alpha$ radiation (0.710 73 Å). A total of 9500 reflections were measured; 1952 reflections were unique ($R_{\text{int}} = 0.0411$), and 1551 reflections with $I > 2\sigma(I)$ were considered to be observed for purposes of *R* value computation. The data were corrected for Lorentz and polarization factors. A summary of data collection parameters is given in Table 1.

The structure was solved by direct methods. It was immediately obvious from refinement of the unique halide position that a minor Br impurity was present. The disorder was not resolvable, and the crystallographic position was refined with partial Cl and Br occupancy. The occupancy factors were refined to values of 0.8 for Br and 1.2 for Cl. In addition to the disorder mentioned above, one N–Et group was fractionally disordered across a mirror plane. Both N1 and C5 (Figure 1) were refined at 50% occupancy just off the mirror site. The terminal methyl group (C6) resided on the mirror and was not disordered. Although lowering the symmetry to *Pnm2*₁ would remove the mirror plane, only N1 and C5 would be affected. Thus, when this was attempted, the remaining mirror related atoms showed high correlations and would not refine properly. Electron density consistent with the N1, C5 disorder was also still present. The symmetry was returned to *Pnma* and the refinement completed in this space group. The geometrically constrained hydrogen atoms were placed in calculated positions and allowed to ride on the bonded atom with $B = 1.2U_{\text{eqv}}(\text{C})$. The methyl hydrogen atoms were included as a rigid group with rotational freedom at the bonded carbon atom ($B = 1.2U_{\text{eqv}}(\text{C})$). The remaining three hydrogen atoms were located from a difference Fourier map and

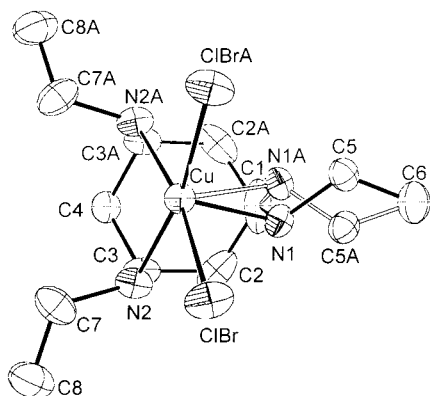


Figure 1. ORTEP view of $[\text{Cu}(\text{tach-Et}_3)\text{Br}_{0.8}\text{Cl}_{1.2}]$ showing mirror disorder (50% probability ellipsoids). The A-suffixed atoms are generated by crystallographic mirror symmetry. Atoms N1A and C5A are also disordered with N1 and C5 about the plane. Hydrogens have been omitted for clarity.

allowed to ride on the bonded N atoms with $B = 1.2U_{\text{eq}}(\text{N})$. Refinement of the non-hydrogen atoms was carried out with anisotropic temperature factors. Final values of $R(\text{all data}) = 0.0596$, $R_w(\text{all data}) = 0.1000$, $R(\text{obs data}) = 0.0413$, and $R_w(\text{obs data}) = 0.0900$ were obtained with a GOF (on F^2) of 1.070 and SHELX-93 weight parameters of 0.0461 and 1.3522.

Results

Ligand Syntheses. The tach-Pr₃ derivative was prepared as the trihydrobromide salt by modification of the syntheses of previously reported tach,¹⁹ tach-Me₃, and tach-Et₃.²⁰ The sterically bulky neopentyl and the 2-furanylmethyl derivatives were synthesized analogously to the 2-thienylmethyl derivative, tach-thioph₃,¹⁸ by formation of the triimine followed by reduction with excess borohydride. This route obviated concerns about acid-promoted rearrangements of the neopentyl group as well as steric challenges to alkylation that could arise in the method employed for tach-Me₃ and tach-Et₃.²⁰

Cu(II) Complex Syntheses. The complexes $[\text{Cu}(\text{tach-R}_3)\text{Cl}_2]$ were prepared from the appropriate copper salts and free triamines in analogy to the previously reported $[\text{Cu}(\text{tach-thioph}_3)\text{Cl}_2]$.¹⁸ In one case, tach-Me₃·3HBr was not fully converted to the free triamine and the remaining trace of bromide ions resulted in the mixed anion product $[\text{Cu}(\text{tach-Et}_3)\text{Br}_{0.8}\text{Cl}_{1.2}]$, which was structurally characterized. Subsequently, $[\text{Cu}(\text{tach-Et}_3)\text{Cl}_2]$ was prepared and used for further studies; it was demonstrated that all relevant properties of the two substances were identical.

Attempts to prepare $[\text{Cu}(\text{tach-neopentyl}_3)\text{Cl}_2]$ thus far have yielded impure materials of poor solubility. The steric effect of neopentyl groups may serve to energetically bias this ligand toward the N₃-trisequatorial conformation, preventing formation of a discrete complex and instead favoring a polymeric structure with each copper bound to multiple, bridging tach ligands.

In situ preparation of aqueous $[\text{Cu}(\text{tach-R}_3)]^{2+}$ ($\text{R} = \text{Me}, \text{Et}$) was accomplished by adding a slight excess (<1%) of tach-R₃(aq) to $\text{CuCl}_2(\text{aq})$ at pH 7. At concentrations above ca. 1 mM, precipitation of uncharacterized blue solids occurred outside the pH range 6.71 to 11.22 or in the absence of a slight excess of ligand. The Cu(II) complexes of other tach-R₃ ($\text{R} = n\text{-Pr}, \text{CH}_2\text{-2-thienyl}, \text{and } \text{CH}_2\text{-2-furanyl}$) were solubilized by MeOH as cosolvent. Attempts to obtain an accurate base titration of a mixture of tach-R₃·3HBr and $\text{Cu}^{2+}(\text{aq})$ in order to determine pK_a 's and stability constants were not successful, due to the limitations of pH range and solubility in this system.

Table 2. Selected Bond Lengths (Å) and Angles (deg) of $[\text{Cu}(\text{tach-Et}_3)\text{Br}_{0.8}\text{Cl}_{1.2}]$

Cu–N(2)	2.053(2)	Cu–N(1)	2.218(5)
Cu–ClBr	2.3948(6)	N(1)–C(5)	1.478(7)
N(1)–C(1)	1.524(6)	N(2)–C(7)	1.484(4)
N(2)–C(3)	1.498(4)	C(1)–C(2)	1.519(5)
C(2)–C(3)	1.517(5)	C(3)–C(4)	1.515(4)
C(5)–C(6)	1.528(7)	C(7)–C(8)	1.506(5)
N(2)–Cu–N(2A) ^a	91.98(14)	N(2)–Cu–N(1A) ^a	96.75(14)
N(2)–Cu–N(1)	83.94(14)	N(2)–Cu–ClBr	86.24(7)
N(2A) ^a –Cu–ClBr	167.63(8)	N(1A) ^a –Cu–ClBr	108.42(12)
N(1)–Cu–ClBr	95.24(12)	ClBr–Cu–ClBr(A) ^a	92.89(3)
C(5)–N(1)–C(1)	109.6(4)	C(5)–N(1)–Cu	111.0(3)
C(1)–N(1)–Cu	109.5(3)	C(7)–N(2)–C(3)	114.2(2)
C(7)–N(2)–Cu	111.7(2)	C(3)–N(2)–Cu	115.7(2)
C(2)–C(1)–C(2A) ^a	110.2(4)	C(2)–C(1)–N(1)	99.7(3)
C(2)–C(1)–N(1A) ^a	122.6(3)	C(3)–C(2)–C(1)	114.6(3)
N(2)–C(3)–C(4)	112.0(3)	N(2)–C(3)–C(2)	110.7(3)
C(4)–C(3)–C(2)	110.9(3)	C(3A) ^a –C(4)–C(3)	112.9(4)
N(1)–C(5)–C(6)	113.0(4)	N(2)–C(7)–C(8)	114.7(3)

^a Equivalent atoms with the suffix "A" are generated by the symmetry transformation $x, -y + 1/2, z$.

Structural Study of $[\text{Cu}(\text{tach-Et}_3)\text{Br}_{0.8}\text{Cl}_{1.2}]$. The $[\text{Cu}(\text{tach-Et}_3)\text{Br}_{0.8}\text{Cl}_{1.2}]$ molecule resides on a crystallographic mirror plane that generates the atoms N2A, ClBrA, C3A, C2A, C7A, and C8A (Figure 1). Fractional disorder of one N–CH₂ group about the mirror plane generates the atom pairs (N1, N1A) and (C5, C5A). Selected bond distances and angles are in Table 2. The metal coordination sphere is nearly square pyramidal, with the N1/N1A position in the apical coordination site and N2, N2A and the halides forming the square base (Figure 1). The apical atom (N1/N1A) deviates slightly from square pyramidal geometry, which may be an artifact of the disorder. However, a distorted square pyramidal coordination sphere is supported by EPR and optical data (see below). The deviation is such that the Cu–N1 or Cu–N1A bond axis is not normal to the N₂X₂ plane. This structure contrasts with that of $[\text{Cu}(\text{tach-thioph}_3)\text{Cl}_2]$ whose Cu coordination sphere distorts toward trigonal bipyramidal geometry.¹⁸ The apical bond distance Cu–N(1) of 2.218(5) Å is longer than the basal one (2.053(2) Å), as is typical of Jahn–Teller-distorted Cu(II). This Cu–N_{apical} bond length is slightly shorter than that of $[\text{Cu}(\text{tach-thioph}_3)\text{Cl}_2]$ (2.288(3) Å), which might be ascribed to a steric effect or again to disorder effects. The Cu–N_{apical} bond also appears marginally shorter than those of $\text{Cu}([\text{9}]\text{aneN}_3)\text{Cl}_2$ ²⁵ and $\text{Cu}([\text{9}]\text{aneN}_3)\text{Br}_2$,²⁶ which are 2.246(4) and 2.231(4) Å, respectively. The Cu–N_{basal} distance of the title compound (2.053(2) Å) is comparable to all distances of $\text{Cu}[(\text{tach-thioph}_3)\text{Cl}_2]$, $\text{Cu}([\text{9}]\text{aneN}_3)\text{Cl}_2$,²⁵ and $\text{Cu}([\text{9}]\text{aneN}_3)\text{Br}_2$ ²⁶ (range 2.038(4)–2.069(3) Å).

The torsion angles C–C–C–C of the cyclohexyl ring, a measure of ligand distortion induced by the metal pushing the nitrogens outward^{27,28} are the following: C(2A)–C(1)–C(2)–C(3), 50.6(5)°; C(1)–C(2)–C(3)–C(4), 52.6(4)°; C(2)–C(3)–C(4)–C(3A), 53.4(4)°. These are not significantly different from those of $\text{Cu}[(\text{tach-thioph}_3)\text{Cl}_2]$, which range from 48.23(41) to 55.29(39)°.¹⁸ There are no significant intermolecular contacts in the structure.

(24) Brand, U.; Vahrenkamp, H. *Inorg. Chim. Acta* **1992**, 198–200, 663.

(25) Schwindinger, W. F.; Fawcett, T. G.; Lalancette, R. A.; Potenza, J. A.; Schugar, H. J. *Inorg. Chem.* **1980**, 19, 1379.

(26) Bereman, R. D.; Churchill, M. R.; Schaber, P. M.; Winkler, M. E. *Inorg. Chem.* **1979**, 18, 3122.

(27) Hilfiker, K. A.; Rogers, R. D.; Brechbiel, M. W.; Planalp, R. P. *Inorg. Chem.* **1997**, 36, 4600.

(28) Choquette, D. M.; Buschmann, W. E.; Olmstead, M. M.; Planalp, R. P. *Inorg. Chem.* **1993**, 32, 1062.

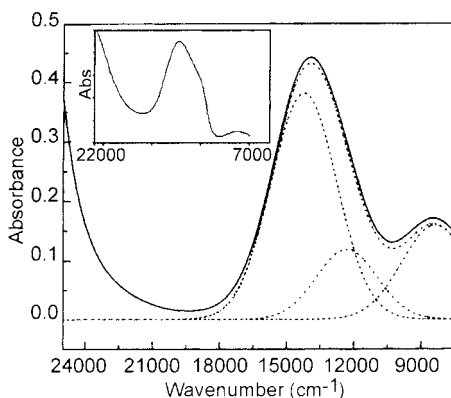


Figure 2. Visible/near-infrared spectra of $[\text{Cu}(\text{tach-Et}_3)\text{Cl}_2]$. The solution-phase spectrum (MeOH, 5 mM) has been simulated (see text). The experimental curve (solid line) is offset by +0.01 absorbance units in order to show the match with the simulated curve (dotted line). The inset depicts the solid-phase spectrum.

Electronic Spectroscopy. Figure 2 shows the visible/near-infrared spectrum of the $[\text{Cu}(\text{tach-Et}_3)\text{Cl}_2]$ complex in MeOH; very similar spectra were obtained for all of the complexes in methanol and aqueous buffer except that the bands were shifted to higher energy in water. The spectra could be satisfactorily fitted to a sum of three Gaussian functions $\epsilon(\nu)$ of the form $\epsilon(\nu) = \epsilon_{\text{max}} \exp[-(\ln 2)4(\nu_{\text{max}} - \nu)^2/\Delta\nu_{1/2}^2]$, where ϵ_{max} and ν_{max} are the molar absorptivity and frequency (cm^{-1}) of the maximum absorption and $\Delta\nu_{1/2}$ is the full width at half-height of the absorption band. Oscillator strengths, f , were calculated from the relationship $f = 4.33 \times 10^{-9} \int \epsilon(\nu) d\nu$.²⁹ Spectral data for the complexes in HEPES buffer and in MeOH are summarized in Table 3 as well as data for solid $[\text{Cu}(\text{tach-Et}_3)\text{Cl}_2]$. We assign the three Gaussian bands to the metal-based $d_{x^2-y^2} \rightarrow d_{z^2}$, d_{xy} , $d_{xz,yz}$ transitions (electron hole formalism) in order of increasing energy as per the work of Duggan et al. on square pyramidal copper complexes.³⁰ The molar absorptivities ~ 10 – $80 \text{ M}^{-1} \text{ cm}^{-1}$ and oscillator strengths $\sim 0.2 \times 10^{-6}$ – 6.5×10^{-6} (Table 3) are typical of d–d bands of square pyramidal copper^{30,31} and of transition ion complexes where parity-forbidden Laporte selection rules are relaxed by lowered symmetry.²⁹ The $d_{x^2-y^2} \rightarrow d_{z^2}$ transition at $\sim 8500 \text{ cm}^{-1}$ is near the low end of ligand field transition energies seen for Cu(II) complexes and reflects the relatively strong axial component of the ligand field produced by the apical nitrogen (N1/N1A in Figure 1) of the complex.^{32,33} The band positions of all the complexes in methanol and of the solid-state sample of $[\text{Cu}(\text{tach-Et}_3)\text{Cl}_2]$ (Figure 2) are similar (Table 3), suggesting that the complexes in methanol and the solid state have essentially the same structure. However, in aqueous media, the bands are approximately 1000 cm^{-1} higher in energy, indicating that a structural change has occurred. We attribute the blue shift to the replacement of Cl^- by the stronger field ligand H_2O in the first coordination sphere. This interpretation is further supported by EPR data and bonding parameters derived below and is consistent with the preference of Cu(II) for H_2O over Cl^- as a ligand. We therefore write the formula for this complex in aqueous solution as $[\text{Cu}(\text{tach-Et}_3)(\text{H}_2\text{O})_2]^{2+}$.

EPR Spectroscopy. Figures 3–6 illustrate the EPR spectra of the various complexes at X-band (9.15 GHz) and Q-band (35 GHz) microwave frequencies. The Q-band spectrum (Figure 3) of the powdered sample of $[\text{Cu}(\text{tach-Et}_3)\text{Cl}_2]$ shows near axial magnetic symmetry with a small in-plane anisotropy, namely $g_x = 2.061$, $g_y = 2.071$, and $g_z = 2.262$, consistent with the distorted square pyramidal structure of the complex (Figure 1). The X-band solution frozen aqueous solution spectra at 77 K of all the complexes prepared with natural abundance $^{63,65}\text{Cu}$ ($I = 3/2$) are very similar (Figure 4) as are their visible-near-infrared spectra (Table 3), indicating essentially identical first coordination spheres for all of them. The same spectra are observed whether pure solid is dissolved in buffer or the complex is prepared in situ from CuCl_2 and ligand. The ^{63}Cu EPR spectra at X-band are characteristic of monomeric copper species in solution. Because the low-field parallel lines are rather broad, $\Delta B_{1/2} \sim 7 \text{ mT}$, they show no evidence of ligand ^{14}N ($I = 1$) superhyperfine couplings (Figure 4), even for samples prepared with isotopically pure ^{63}Cu or with D_2O solvent in which the parallel lines are slightly sharpened. Basal ^{14}N superfine splittings are typically only 1.0–1.5 mT for square pyramidal Cu(II) complexes, and apical nitrogen couplings are much less, $\sim 0.25 \text{ mT}$,^{34–36} and would not be resolved in the spectrum.

Q-band spectra (Figure 5) were measured to resolve the intense perpendicular region of the X-band spectra (Figure 4) into the principal g -factor components. The four ($m_l = \pm 3/2, \pm 1/2$) copper hyperfine parallel lines are fully separated from the perpendicular line at the higher frequency, but there is no evidence of in-plane x,y -anisotropy in g or in the ^{63}Cu hyperfine coupling within the width of the intense perpendicular EPR line (Figure 5). An in-plane g -anisotropy of $g_y - g_x = 0.010$ comparable to that seen for the solid $[\text{Cu}(\text{tach-Et}_3)\text{Cl}_2]$ sample (Figure 3) would not be resolved within the peak-to-peak width, $\Delta B_{\text{pp}} = 10.5 \text{ mT}$, of the perpendicular line of the Q-band spectrum of the complexes (Figure 5).

The frozen solution spectra were analyzed according to the simplified spin Hamiltonian, $H = g_{\parallel}\beta B_z S_z + g_{\perp}\beta(B_x S_x + B_y S_y) + A_{\parallel}S_z I_z + A_{\perp}(S_x I_x + S_y I_y)$. Here all of the symbols have their usual meanings. A_{\perp} , which is not resolved in the frozen solution spectra, was back-calculated from the value of A_{\parallel} determined from the room-temperature spectra in Figure 6, i.e., $A_{\parallel} = A_{\perp}/3 + 2A_{\perp}/3$, assuming the same sign for all of the couplings. The spin Hamiltonian parameters for all of the complexes are summarized in Table 4. Second-order corrections were applied to the X-band spectra but were not required at Q-band. Spin Hamiltonian parameters for the $[\text{Cu}(\text{tach-Et}_3)\text{Cl}_2]$ complex in methanol are not reported since only a broad relatively featureless EPR spectrum (not shown) was obtained in frozen solution at X-band and Q-band, suggestive of solute aggregation upon freezing the sample.

The room-temperature EPR spectra depicted in Figure 6 show increased line broadening with molecular weight that we attribute to the longer rotational correlation times of the larger complexes.³⁷ The close correspondence between g_{\parallel} obtained directly from the room-temperature spectrum and that calculated from the frozen aqueous solution spectrum via the equation $g_{\parallel} = g_{\parallel}/3 + 2g_{\perp}/3$ (Table 4) suggests that the structures of the

(29) Figgis, B. N. *Introduction to Ligand Fields*; Wiley: New York, 1966; p 208.

(30) Duggan, M.; Ray, N.; Hathaway, B.; Tomlinson, A. A. G.; Brint, P.; Pelin, K. *J. Chem. Soc., Dalton Trans.* **1980**, 1342.

(31) Karlin, K. D.; Hayes, J. C.; Juen, S.; Hutchinson, J. P.; Zubieta, J. *Inorg. Chem.* **1982**, *21*, 4106.

(32) Hathaway, B. J.; Billing, D. E. *Coord. Chem. Rev.* **1970**, *5*, 143.

(33) Hathaway, B. J.; Tomlinson, A. A. G. *Coord. Chem. Rev.* **1970**, *5*, 1.

(34) He, Q. Y.; Mason, A. B.; Woodworth, R. C.; Tam, B. M.; MacGillivray, R. T. A.; Grady, J. K.; Chasteen, N. D. *Biochemistry* **1997**, *36*, 14853.

(35) Atherton, M. M.; Horsewill, A. J. *J. Chem. Soc., Faraday Trans.* **1980**, *660*.

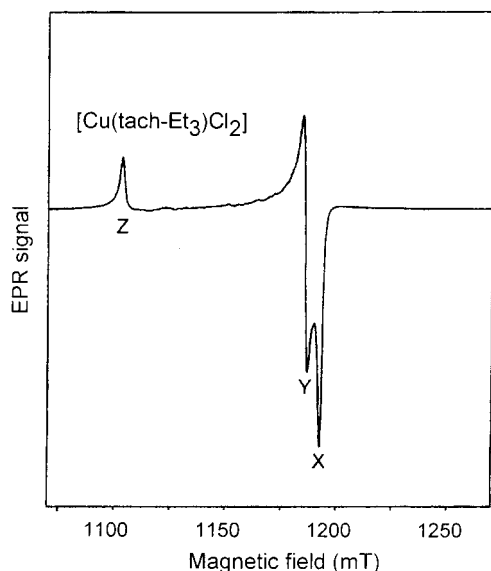
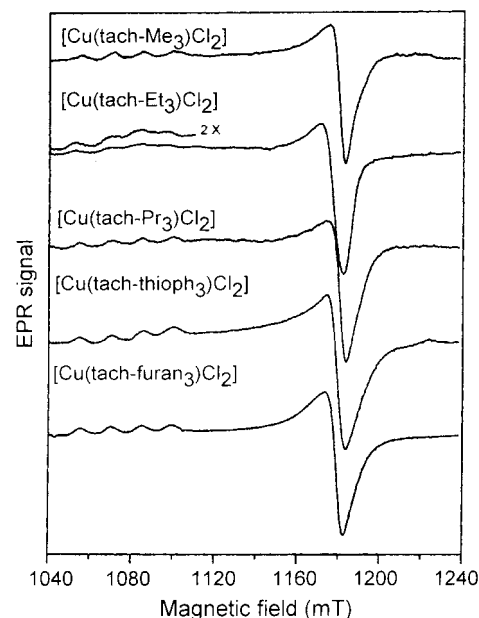
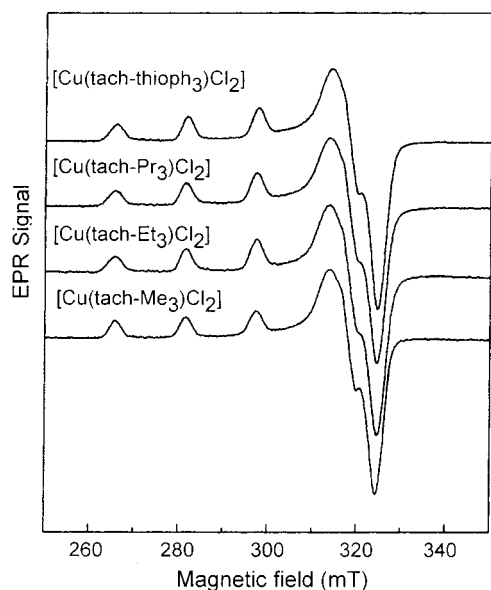
(36) Camp, H. L. V.; Sands, R. H.; Fee, J. A. *J. Chem. Phys.* **1981**, *75*, 2098.

(37) Chasteen, N. D.; Hanna, M. W. *J. Phys. Chem.* **1972**, *76*, 3951.

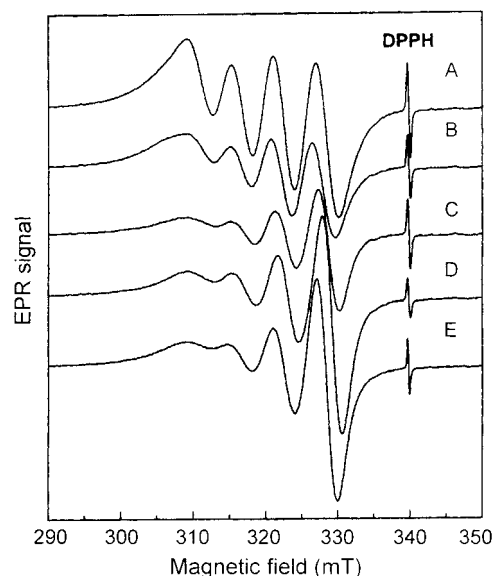
Table 3. Assignments for the Optical Spectra of Cu(II) Complexes of tach-R₃^a

complexes	$\Delta E_{x,y,z}^b$	ΔE_{xy}^b	ΔE_z^b
[Cu(tach-Me ₃)Cl ₂] in MeOH	14 252 (76.2, 6.07)	12 316 (24.4, 1.79)	8388 (31.8, 2.57)
[Cu(tach-Et ₃)(H ₂ O) ₂] ²⁺ in HEPES	14 972 (54.4, 5.94)	12 594 (17.8, 0.25)	9580 (22.0, 1.88)
[Cu(tach-Et ₃)Cl ₂] in MeOH	14 252 (76.2, 6.07)	12 321 (23.8, 1.75)	8398 (31.8, 2.57)
[Cu(tach-Et ₃)Cl ₂] powder	14 496	12 544	8223
[Cu(tach-Pr ₃)Cl ₂] in MeOH	14 482 (75.0, 6.42)	12 491 (19.4, 1.52)	8588 (31.8, 2.58)
[Cu(tach-furan ₃)Cl ₂] in MeOH	14 472 (56.2, 4.48)	12 481 (11.8, 0.92)	8698 (26.2, 0.21)
[Cu(tach-thioph ₃)Cl ₂] in MeOH	14 892 (43.0, 3.96)	12 656 (4.4, 0.43)	9128 (19.2, 1.61)

^a Band maxima in cm⁻¹ from Gaussian fitting of the absorption spectra. Errors nominally ± 10 cm⁻¹. Molar absorptivities (M⁻¹ cm⁻¹) and oscillator strengths (10^{-6}), respectively, in parentheses. ^b $E_{x,y,z} = E_{x^2-y^2} - E_{x,y,z}$; $\Delta E_{xy} = E_{x^2-y^2} - E_{xy}$; $\Delta E_z^2 = E_{x^2-y^2} - E_z^2$.

**Figure 3.** Q-band EPR spectrum of powdered [Cu(tach-Et₃)Cl₂] at room temperature.**Figure 5.** Q-band EPR spectra of [Cu(tach-R₃)]²⁺(aq) in frozen (100 K) HEPES/glycerol buffer, pH 7.4.**Figure 4.** X-band EPR spectra of [Cu(tach-R₃)]²⁺(aq) in frozen (77 K) HEPES/glycerol buffer, pH 7.4.

complexes in water are essentially the same in the liquid and frozen states. In general, the spin Hamiltonian parameters are very similar for all of the tach complexes in aqueous media (Table 4), including that of tach-thioph₃, whose Cu(II) structure has been previously determined.¹⁸ We conclude that steric effects from substituents on the coordinating nitrogens do not significantly alter the first coordination sphere structure of any of the complexes. Moreover, the similarity in the spin Hamiltonian

**Figure 6.** X-band EPR spectra of [Cu(tach-R₃)]²⁺(aq) in room-temperature HEPES buffer, pH 7.4. A–E correspond to Cu(II) complexes of ligands tach-R₃, R = Me, Et, *n*-Pr, thioph, and furan, respectively. DPPH is the *g*-mark standard (*g* = 2.0037) diphenylpicrylhydrazyl radical.

parameters of the *N*-ethyl compound in pH 7.4 and pH 10.1 solutions (Table 4) indicates that the complex does not undergo appreciable hydrolysis at the higher pH. In general, all of the spectra are consistent with the presence of one major species

Table 4. Spin Hamiltonian Parameters^a

copper complexes	g_0	g_{\parallel}	g_{\perp}	A_0 (10^{-4} cm ⁻¹)	A_{\parallel} (10^{-4} cm ⁻¹)	A_{\perp} (10^{-4} cm ⁻¹) ^c
[Cu(tach-Me ₃)(H ₂ O) ₂] ²⁺ ^d	2.127	2.264	2.066	58.0	166.9	3.5
[⁶³ Cu(tach-Me ₃)(H ₂ O) ₂] ²⁺ ^d	2.132 ^e	2.265	2.066		164.2	
[Cu(tach-Et ₃)(H ₂ O) ₂] ²⁺ ^d	2.128	2.266	2.066	55.5	164.3	1.2
[Cu(tach-Et ₃)(H ₂ O) ₂] ²⁺ ^f	2.128 ^e	2.263	2.061		165.0	
[Cu(tach-Et ₃)Cl ₂] powder ^b	2.131 ^g	$g_z = 2.262$	$g_x = 2.061$ $g_y = 2.071$			
[Cu(tach-Pr ₃)(H ₂ O) ₂] ²⁺ ^d	2.127	2.266	2.065	59.3	164.6	6.7
[Cu(tach-furan ₃)(H ₂ O) ₂] ²⁺ ^d	2.127	2.261	2.064	58.8	164.0	6.2
[Cu(tach-thioph ₃)(H ₂ O) ₂] ²⁺ ^b	2.124	2.261	2.063	60.5	165.7	8.0

^a g values have errors of ± 0.001 , and hyperfine couplings have errors of $\pm 0.2 \times 10^{-4}$ cm⁻¹. Anisotropic parameters were measured from Q-band spectra of frozen solutions at Q-band frequency at 100 K, and isotropic parameters, from X-band spectra of room-temperature solutions. ^b The [Cu(tach-Et₃)Cl₂] powder sample displayed rhombic symmetry in its g -values (Figure 3). ^c A_{\perp} values were calculated from $A_0 = 1/3A_{\parallel} + 2/3A_{\perp}$. ^d 5 mM complex in 50 mM HEPES buffer, pH = 7.4. ^e Calculated from the relationship $g_0 = 1/3g_{\parallel} + 2/3g_{\perp}$. ^f 2.5 mM complex in 50 mM CAPS buffer, pH = 10.1. ^g Calculated from the relationship $g_0 = 1/3(g_x + g_y + g_z)$.

in solution. Since $g_{\parallel} > g_{\perp} > 2.0$, the ground-state orbital containing the unpaired electron corresponds to $d_{x^2-y^2}$ as expected for a square-pyramidal structure with a Jahn–Teller axial elongation.³⁸

Bonding Parameters. The LCAO-MO bonding parameters of the [Cu(tach-Et₃)]²⁺ in aqueous media were calculated from the optical transitions and the EPR spin Hamiltonian parameters (Tables 3 and 4) using the classic equations of Maki and McGarvey.³⁹ A free Cu(II) ion spin–orbit coupling constant $\lambda = -868$ cm⁻¹, Fermi contact term $k_0 = 0.43$, $d_{x^2-y^2}$ ground-state dipole term $P = 0.036$ cm⁻¹, and $T(n)_{\text{nitrogen}} = 0.33$ and $T(n)_{\text{oxygen}} = 0.220$ were assumed.⁴⁰ The small terms in $T(n)$ in the bonding parameter equations³⁹ reflect the orbital hybridization about the donor atoms, and the results are not very sensitive to the value chosen for $T(n)$; they are frequently ignored in bonding parameter calculations. The calculation yields α^2 , β^2 , and β_1^2 , the squares of MO coefficients of the metal-centered $d_{x^2-y^2}$, $d_{xz,yz}$, and d_{xy} orbitals, respectively. α^2 represents the fractional unpaired electron density in the ground state wave function. Because of uncertainties in such calculations, only the relative values of the bonding parameters are useful; lower values of α^2 , β^2 , and β_1^2 correspond to increased “covalency.” The calculated value for $\alpha^2 \sim 0.78$ indicates moderate in-plane σ -bond covalency involving the ground-state $d_{x^2-y^2}$ orbital and is typical of many square pyramidal complexes of copper(II).^{32,33,39,40,41} On the other hand, the computed values of $\beta^2 \sim 0.92$ and $\beta_1^2 \sim 0.88$ are indicative of rather ionic out-of-plane and in-plane π -bonding involving the $d_{xz,yz}$ and d_{xy} orbitals, respectively. The ionic character of the π -bonds is consistent with the replacement of Cl⁻ by H₂O in the equatorial plane of the complex. While chloride can readily participate in π -bonding,³² both water and the donor nitrogen atoms of the tach ligand lack orbitals with appropriate symmetry for effective π -bonding. Considerable ionic character in the π -bonding is therefore expected for [Cu(tach-Et₃)(H₂O)₂]²⁺, as observed.

Discussion

Copper complexes with open coordination sites have catalytic activity in many reactions that are relevant to biology^{7,42,43} and organic synthesis.^{2,3} The present studies focus on the nature of

L–Cu(II)–aquo and L–Cu–hydroxo species (L = triamine ligand) that may be active species in hydrolysis reactions or other Lewis-acid-catalyzed processes. The goal of these studies is to understand structure and speciation of Cu(II) complexes that may lead to mechanistic insight into the hydrolysis process and more effective hydrolysis agents. Structures of copper catalyst precursors and active species have been elucidated by spectroscopic methods with some success in the Cu^{II}([9]-aneN₃)²⁺^{10,44} and Cu^{II}(tach-H₃)²⁺¹⁴ systems for hydrolytic cleavage of phosphate diesters (particularly bis(*p*-nitrophenyl) phosphate (BNPP), a model for nucleotide cleavage). A commonly postulated rate-determining step in metal-promoted phosphate diester or amide cleavage is the transfer of a coordinated hydroxo group to the respective phosphorus or amide carbon.

We have observed that a Cu(II) complex of tach-Me₃ may be readily formed in situ at pH 7.4 from aqueous Cu(II) and tach-Me₃. The resulting solutions are active in cleavage of BNPP at relatively high rates, by a process that is unusual because it is second-order in concentration of copper complex.¹⁵ Therefore, we wish to understand the structure, bonding, and reactivity issues of isolated and solution-phase complexes of Cu(II) with tach-R₃. It was also of interest to know the effects of variation of R in this system. In the Cu(II)–[9]aneN₃ system, it has been observed that addition of *i*-Pr groups to nitrogen changes the position of a monomer–dimer equilibrium of the Cu(II) complexes, presumably through a steric effect.⁴⁵ It is believed that only the monomeric Cu(II)–hydroxo species is active in the catalytic process; therefore, the position of this equilibrium affects the rate of hydrolysis.^{7,10}

The solid-state structure of [Cu(tach-Et₃)Br_{0.8}Cl_{1.2}] is a distorted square-based pyramid in which the two halides occupy basal positions. Structures of copper(II) triamino dihalide complexes typically vary from square-based pyramidal to trigonal-bipyramidal in the solid state.³² For example, complexes [Cu([*n*]aneN₃)X₂] ($n = 9$, X = Cl, Br) possess the square-based pyramidal geometry, but distortions occur as n increases to 11, where the shape of [Cu([11]aneN₃)Br₂] is closer to trigonal-bipyramidal. All of these complexes are active hydrolysis catalysts, and there is no observed relationship of coordination geometry to hydrolytic ability.⁴⁶

The displacement of coordinated halide from [Cu(tach-R₃)Cl₂] is important to the catalytic activity of the complexes, for it provides labile coordination sites for substrate binding.⁷ We

(38) Pilbrow, J. R. *Transition Ion Electron Paramagnetic Resonance*; Clarendon Press: Oxford, U.K., 1990; p 624.

(39) Maki, A. H.; McGarvey, B. R. *J. Chem. Phys.* **1958**, *29*, 31.

(40) Kivelson, D.; Neiman, R. *J. Chem. Phys.* **1961**, *35*, 149.

(41) Gersmann, H. R.; Swalen, J. D. *J. Chem. Phys.* **1961**, *36*, 3221.

(42) Karlin, K. D.; Zubieta, J., Eds.; *Copper Coordination Chemistry: Biochemical and Inorganic Perspectives*; Adenine Press: Guilderland, NY, 1983.

(43) Comba, P. *Coord. Chem. Rev.* **2000**, in press.

(44) Deal, K. A.; Hengge, A. C.; Burstyn, J. N. *J. Am. Chem. Soc.* **1996**, *118*, 1713.

(45) Burstyn, J. N. Personal communication.

(46) Hegg, E. L.; Mortimore, S. H.; Cheung, C. L.; Huyett, J. E.; Powell, D. R.; Burstyn, J. N. *Inorg. Chem.* **1999**, *38*, 2961.

addressed the question of whether the copper-halide bond hydrolysis could be observed in solution by characterizing the structure of tach-R₃ complexes of Cu(II) in both MeOH and buffered aqueous phases. Dissolving [Cu(tach-Et₃)Br_{0.8}Cl_{1.2}] in MeOH gives a square-pyramidal complex of the same structure as the crystalline material, according to UV-vis spectroscopy. The spectroscopy further demonstrates that in MeOH, all of the complexes [Cu(tach-R₃)Cl₂] (R = Me, Et, *n*-Pr, CH₂-2-thienyl, CH₂-2-furanyl) share the square-bipyramidal structure with a d_{x²-y²} ground state, and halide remains bound.

We examined the aqueous-phase reactivity of [Cu(tach-R₃)-X₂] in detail with a combined application of EPR spectroscopy (X- and Q-band) and UV-vis spectroscopy. When [Cu(tach-Et₃)X₂] is dissolved in buffered aqueous medium at pH 7.4, the hydrolysis of copper-halide bonds is observed. An increase in ligand field strength is noted in the shift of the UV-vis bands in [Cu(tach-Et₃)]²⁺(aq) relative to the dihalide. Further, the copper orbital bonding parameters derived for [Cu(tach-Et₃)]²⁺(aq) show rather ionic bonding. Both of these findings are consistent with replacement of halide by water to afford [Cu(tach-Et₃)(H₂O)₂]²⁺. Further, all of the [Cu(tach-R₃)X₂] complexes similarly exhibit hydrolysis. The same spectroscopic parameters are observed for the complex formed in situ from CuCl₂(aq) and tach-Me₃·3HBr. In total, these findings imply that the solution speciation of [Cu(tach-R₃)(H₂O)₂]²⁺ is a reasonable formulation of the catalyst precursors. The EPR data also indicate a similar aqueous speciation of all the tach-R₃-copper compounds (R = Me, Et, *n*-Pr, CH₂-furanyl, and CH₂-thienyl) (Table 4).

Variation of ligand bound to Cu(II) is known to affect the activity of the catalyst in hydrolytic reactions, for example as demonstrated in the homologous complexes [Cu(*n*)aneN₃)X₂] (*n* = 9, 10, 11).⁴⁶ However, there was little or no effect of variation of R on either the coordination geometry or the ligand-field splitting of Cu(II)(tach-R₃) complexes in the present study, even though R varies considerably in steric bulk (R = Me, Et, *n*-Pr, CH₂-2-thienyl, and CH₂-2-furanyl). However, it was observed that a ligand with very large steric bulk, tach-neopentyl₃, reacted with Cu(II) to form an intractable blue material. Possibly in this select case tach-R₃ remains in the open conformation, forming a two-dimensional coordination polymer with Cu(II).

The formation of metal-bound hydroxide has been postulated in studies of mechanism of hydrolysis by numerous metal ions, but the findings with the Cu(II)-tach-R₃ system differ notably from other Cu(II)-triamine compounds studied.^{7,47} In hydrolysis of BNPP by [Cu([9]aneN₃)Cl₂], it is believed that Cl is first displaced by water to afford [Cu([9]aneN₃)(H₂O)₂]²⁺, which then dimerizes to [Cu([9]aneN₃)(μ-OH)]₂²⁺. Then the dimer dissociates to form a small amount of the active complex [Cu([9]-

aneN₃)(H₂O)(OH)]⁺.¹⁰ Burstyn et al. measured an apparent pK_a of [Cu([9]aneN₃)]²⁺(aq) of 7.3 but point out that this value is not a true pK_a because the dimerization equilibrium produces additional proton donor and acceptor species.⁷ In the Cu(II)-tach (i.e., tach-H₃) system, Fujii et al. have proposed that [Cu(tach)(H₂O)(OH)]⁺ forms directly from [Cu(tach)(H₂O)₂]²⁺ at a pK_a of 8.2 ± 0.1 and did not report any evidence for dimeric species.¹⁴ However, the EPR spectra of [Cu(tach-Et₃)(H₂O)₂]²⁺(aq) are identical at pH 7.4 and 10.1, suggesting that a single species prevails in this pH range, i.e., that the pK_a of coordinated water in this complex is above 10.1.⁴ We investigated dimerization of [Cu(tach-Me₃)]²⁺(aq) by quantitative EPR studies at pH 7.4. The presence of a substantial amount (more than ca. 3%) of an EPR-silent, antiferromagnetically coupled Cu(II) dimer was ruled out through comparison of the intensity of the spectrum of [Cu(tach-Me₃)]²⁺(aq) to a Cu(II) standard.¹⁵ Because Cu(II) hydroxo species are predominantly dimers or oligomers in which the hydroxide bridges two metal centers, the inability of [Cu(tach-Me₃)]²⁺(aq) to dimerize suggests it assumes the aquo speciation, [Cu(tach-Me₃)(H₂O)₂]²⁺, as supported by the data reported herein.

Conclusion

The complexation chemistry of Cu(II) with tach-R₃ has been defined in the solid and solution (aqueous pH 7.4 and methanolic) phases. All solid- and solution-phase forms of [Cu(tach-R₃)X₂] appear to share the square-pyramidal structure. In aqueous medium at pH 7.4, coordinated halides are replaced by water to give [Cu(tach-R₃)(H₂O)₂]²⁺. There is no substantial effect of variation of R on the ligand field splitting or coordination geometry in tach-R₃ complexes of Cu(II), as evidenced by the EPR and visible-near-IR spectroscopic data.

Like [9]aneN₃, the Cu(II) complex [Cu(tach-Me₃)(H₂O)₂]²⁺ is an active catalyst in phosphate diester hydrolysis. However, the tach-Me₃ ligand apparently forms a monomeric Cu(II) complex at pH 7.4, in contrast to [9]aneN₃ whose complex is dimeric. Therefore, the mechanism of this hydrolysis process, and its relationship to the aqueous speciation of Cu(II) with tach-R₃, promise to be intriguing and will be taken up in the following paper.¹⁵

Acknowledgment. R.P.P. thanks the NIH for support. F.H.L. thanks the NIH for an STRP fellowship. The authors thank Nole Whittaker (Laboratory of Analytical Chemistry, NIDDK) for his efforts in obtaining FAB-MS spectra for this work. We thank Ms. Ann Przyborowska for the preparation of Figure 2 and Mr. Neng Ye for preparation of [Cu(tach-thioph₃)Cl₂]. This work was supported in part by NIH Grant R37 GM20194 (N.D.C.)

Supporting Information Available: X-ray crystallographic data in CIF format. This material is available free of charge via the Internet at <http://pubs.acs.org>.

IC000829E

(47) Pratiel, G.; Bernadou, J.; Meunier, B. *Adv. Inorg. Chem.* **1998**, *45*, 251.